



# Micro-tensile testing of the bond line in hot isostatic pressed aluminum

April 2022

*Changing the World's Energy Future*

David M Frazer, Fei Teng, Daniel J Murray, Alex N Pomo, Alexander J Winston, James I Cole, Jan-Fong Jue, Jeffrey J Giglio



**DISCLAIMER**

This information was prepared as an account of work sponsored by an agency of the U.S. Government. Neither the U.S. Government nor any agency thereof, nor any of their employees, makes any warranty, expressed or implied, or assumes any legal liability or responsibility for the accuracy, completeness, or usefulness, of any information, apparatus, product, or process disclosed, or represents that its use would not infringe privately owned rights. References herein to any specific commercial product, process, or service by trade name, trade mark, manufacturer, or otherwise, does not necessarily constitute or imply its endorsement, recommendation, or favoring by the U.S. Government or any agency thereof. The views and opinions of authors expressed herein do not necessarily state or reflect those of the U.S. Government or any agency thereof.

# **Micro-tensile testing of the bond line in hot isostatic pressed aluminum**

**David M Frazer, Fei Teng, Daniel J Murray, Alex N Pomo, Alexander J Winston,  
James I Cole, Jan-Fong Jue, Jeffrey J Giglio**

**April 2022**

**Idaho National Laboratory  
Idaho Falls, Idaho 83415**

**<http://www.inl.gov>**

**Prepared for the  
U.S. Department of Energy  
Under DOE Idaho Operations Office  
Contract DE-AC07-05ID14517**

## **Micro-Tensile Testing of the Bond line in Hot Isostatic Pressed Aluminum**

D. Frazer, F. Teng, D. Murray, A. Pomo, A. Winston, J.I. Cole, J.-F. Jue, J. Giglio

Idaho National Laboratory, 2525 Fremont Ave, Idaho Falls, ID USA

### **Abstract**

Considerable effort is being devoted to development and regulatory qualification of low enriched fuels for research and test reactors by many agencies worldwide. One promising fuel configuration being examined for united states higher power research and test reactors (USHPRRs) are plate-type fuels composed of a metallic uranium-molybdenum foil clad in an aluminum alloy. The two pieces of aluminum alloy cladding are bonded using a hot isostatic pressing method. The mechanical properties of the resulting bond line in the aluminum alloy cladding will vary by the HIP'ing parameters requiring a need to characterize the bond line. Small scale mechanical testing can provide a path for evaluating the mechanical properties and deformation behavior of the bond line both prior to and following irradiation. In this research room temperature micro-tensile specimens of non-irradiated and irradiated samples containing an Al alloy (AA 6061) bond line were tested to evaluate its strength and deformation behavior. Observations indicated that the strain rate did not affect the deformation behavior or strength and most of the micro-tensile specimens failed in a ductile mode in grains around the bond line. There was no indication that the microstructural features from the bond line affected the mechanical properties of the micro-tensile specimens. This implies that the bonding process used to make the fuel plate won't be a likely source of failure during irradiation. An initial examination was performed on irradiated material but further systematic studies of the effects of irradiation can be performed in the future.

**Keywords:** Micro-tensile testing, Post irradiation examination, hot isostatic pressing

### **Introduction**

Uranium-molybdenum (U-Mo) alloys are currently being studied to facilitate the conversion of research and test reactors from high enriched fuels to low enriched fuels [1-11]. This program is being administrated by the National Nuclear Security Administration's Material Management and Minimization Reactor Conversion Program (formerly known as the Reduced Enrichment for Research and Test Reactor – RERTR). A fuel core meat design features a monolithic uranium-10 wt.% molybdenum [1-4] fuel configuration, utilizing an aluminum alloy cladding (AA 6061). This design is intended for the use in high performance research reactors (USHPRR) and must provide the minimum required fissile uranium density for their operation before conversion of the test reactor can be implemented. The fuel design clads the fuel core with AA 6061 that is bonded with a hot isostatic pressing (HIP) process which has consistently produced a reliable bond [12, 13].

The HIP process has generally created an adequate bond to date, however a detailed analysis of the mechanical properties and changes in deformation behavior after irradiation of the bond line are still needed to better understand and model its behavior [12, 13]. At the interface of the two AA 6061 sheets a bond line is formed during the HIP process [12]. This bond line can develop a thin oxide layer and form precipitates ( $Mg_2Si$ ) which may affect its bond strength. Evaluating the mechanical properties normal to the bond line is rather difficult due to the thinness of the fuel

plates. This has limited the current research to a few studies employing a variety of techniques which have been able to document the deformation behavior and strength metrics of the bond line [14-18]. A detailed analysis of the mechanical properties of these bond lines is needed to develop better models of the fuel plates' behavior during operation, potential accidents, and long-term storage after use. While testing of the entire fuel plate will produce values about its overall mechanical properties, an understanding of the individual components will provide an evaluation of the interplay between them. This can enable enhanced modeling of the fuel plate and deeper comprehension of the overall fuel plate behavior [19, 20, 21].

Small scale mechanical testing (SSMT) refers to a group of techniques that are used to evaluate the mechanical properties of materials at the micron scale [21, 22]. These techniques permit the manufacture of multiple test specimens using a minute volume of material in as-fabricated components [21,22]. Micro-scale tensile testing can be employed for the evaluation of the mechanical properties of the bond line in as-manufactured HIP process fuel assemblies. Additionally, the small size of the specimens allows for targeting microstructural features in the bond line such as precipitates which may affect the overall strength. Targeting individual microstructural features in the bond line will provide more focused investigations into how each feature affects the overall strength of the fuel plates. The micro size of the specimens is also advantageous in that it enables the manufacturing of multiple specimens with small volumes of material. In Nuclear fuels research this is very desirable for evaluating materials after irradiation allowing the testing to be performed outside of protective hot cells greatly reducing time and expenses. These techniques are beneficial for post irradiation examination as it has been demonstrated that micro-tensile testing of specimens is able to evaluate the change in mechanical properties and deformation behavior of materials after irradiation [23].

In this work micro-tensile fuel specimens were manufactured in a control AA 6061 (not HIP processed) [labeled Al control], HIP processed AA 6061 samples (2 samples) [labeled Al bond line 1 and Al bond line 2] which contained the bond line being studied and one irradiated sample [labeled irradiated]. It was observed in the unirradiated specimens that regardless of notching the bond line most of specimens failed in the aluminum grains on either side of the bond line. There was one micro-tensile specimen in the unirradiated case that failed at the bond line which will be discussed later in this manuscript. Observations also indicated that despite the precipitates being present on the bond line of the micro-tensile specimen, the failure still occurred in the surrounding aluminum grains surrounding the bond line. Due to experimental difficulty with the irradiated sample, only one successful test was completed where the specimen failed at the bond line. While the results from a single test are inconclusive it demonstrates that SSMT can be applied to irradiated materials and allows for some comparison between irradiated and unirradiated conditions.

## **Experimental**

### **Plate Manufacture**

General details of the U-Mo monolithic mini-plate fabrication have been reported previously [24-26]. In general, the U-10wt% fuel foils were fabricated by hot co-rolling a zirconium diffusion

barrier foil to a U-10 wt% Mo coupon at 650°C to a preset thickness followed by cold rolling to the final thickness. Hot isostatic pressing was utilized to bond the AA 6061 cladding to the fuel foil at 560°C and 104 MPa for 90 minutes with a ramping rate of 280°C per hour. The three samples containing bond lines (Al bond line 1, Al bond line 2 and irradiated) were all manufactured by the same parameters described above.

### **Micro-Tensile Fabrication**

A total of 14 successful micro-tensile tests were performed on the 4 samples. On the Al control sample there was 3 test, Al bond line 1 had 6 test, Al bond line 2 had 4 tests and the irradiated sample had 1 test. The manufacturing of the micro-tensile bars smaller sections containing the bond line were cut from the mini fuel plates of the 3 HIP processed samples to fit in the nanoindenters and allow for easier sample preparation of both the unirradiated and irradiated samples. The bond line in each section was located using a Zeiss optical microscope and marked. The samples were then mechanically polished using silicon carbide papers with water as a lubricant until close to the bond line, approximately 100-200  $\mu\text{m}$  away. The polishing was then finished with three and one  $\mu\text{m}$  diamond suspensions. The polishing was also performed on the front of the sample to provide two polished sides enabling the manufacture of the micro-specimens. The control AA 6061 samples were manufactured from a sample of Al cladding that had not been used in the HIP process. It was also polished on two sides using the same process as the HIP samples.

The micro-tensile specimens were manufactured in a FEI Helios plasma focused ion beam (PFIB) located at the irradiated materials characterization laboratory (IMCL) at the Materials and Fuels Complex (MFC) of the Idaho National Laboratory (INL). The advantage of using the PFIB is that this system uses a xenon plasma for the milling instead of gallium ion beam, which is what has typically used in focused ion beam (FIB) systems. The challenge with manufacturing aluminum specimens with gallium FIBs is liquid metal embrittlement of the aluminum at grain boundaries which is remediated by using the xenon plasma [27].

The samples were mounted on a 45° holder allowing for milling perpendicularly into two adjacent surfaces of the sample, which enables the manufacturing of the micro-tensile geometry. A current of 1.3  $\mu\text{A}$  was used to mill the excess material away until approximately 30  $\mu\text{m}$  away from the bond line. This removed sufficient material behind and around the micro-tensile bars to allow the tip of the Hyistron PI-88 picoindenter to reach the specimens as seen in Figure 1.

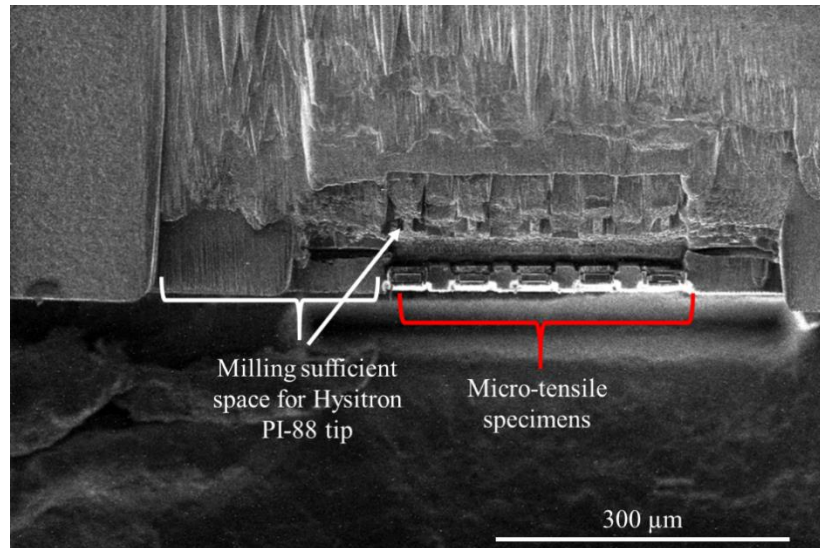


Figure 1: Overview image showing the large amount of milling performed to ensure enough space around the micro-tensile specimens for testing.

To manufacture the micro-tensile specimens, foil structures approximately 20  $\mu\text{m}$  thick, 300  $\mu\text{m}$  in length and 50  $\mu\text{m}$  in height were cleaned (60 nA beam) in each sample with the PFIB at approximately 30  $\mu\text{m}$  from the bond line. When the rough trenching was done, successively lower currents were used to shape the micro-tensile bars with a final cleaning of 6.7 nA. The final dimensions for the micro-tensile bars had a gauge size of  $7 \times 7 \times 20 \mu\text{m}^3$  with a notch causing the width of the micro-tensile specimen to be approximately 3-5  $\mu\text{m}$  at the bond line. An example of a finished micro-tensile bar can be seen in Figure 2B. An ion etched image of the aluminum before manufacturing the tensile bars shows the grains. From the ion etched image it can be seen that grain size is larger than the micro-tensile bars. It is evident that manufactured tensile bars were mostly bi-crystal with a single grain on each side of the bond line. In addition, the micro-tensile bars were over tilted by  $2^\circ$  on the front and back faces during the cleaning to account for the beam broadening, which minimizes the taper on the specimens. The micro-tensile specimens were manufactured with the bond line located near the center of the gauge length. Lastly, the bond line was notched using a circular pattern and a current of 6.7 nA to concentrate the stress at the bond line as seen in Figure 2B. For the micro-tensile specimens manufactured in the control Al (as received) with no bond line the final step of milling the notch was omitted.

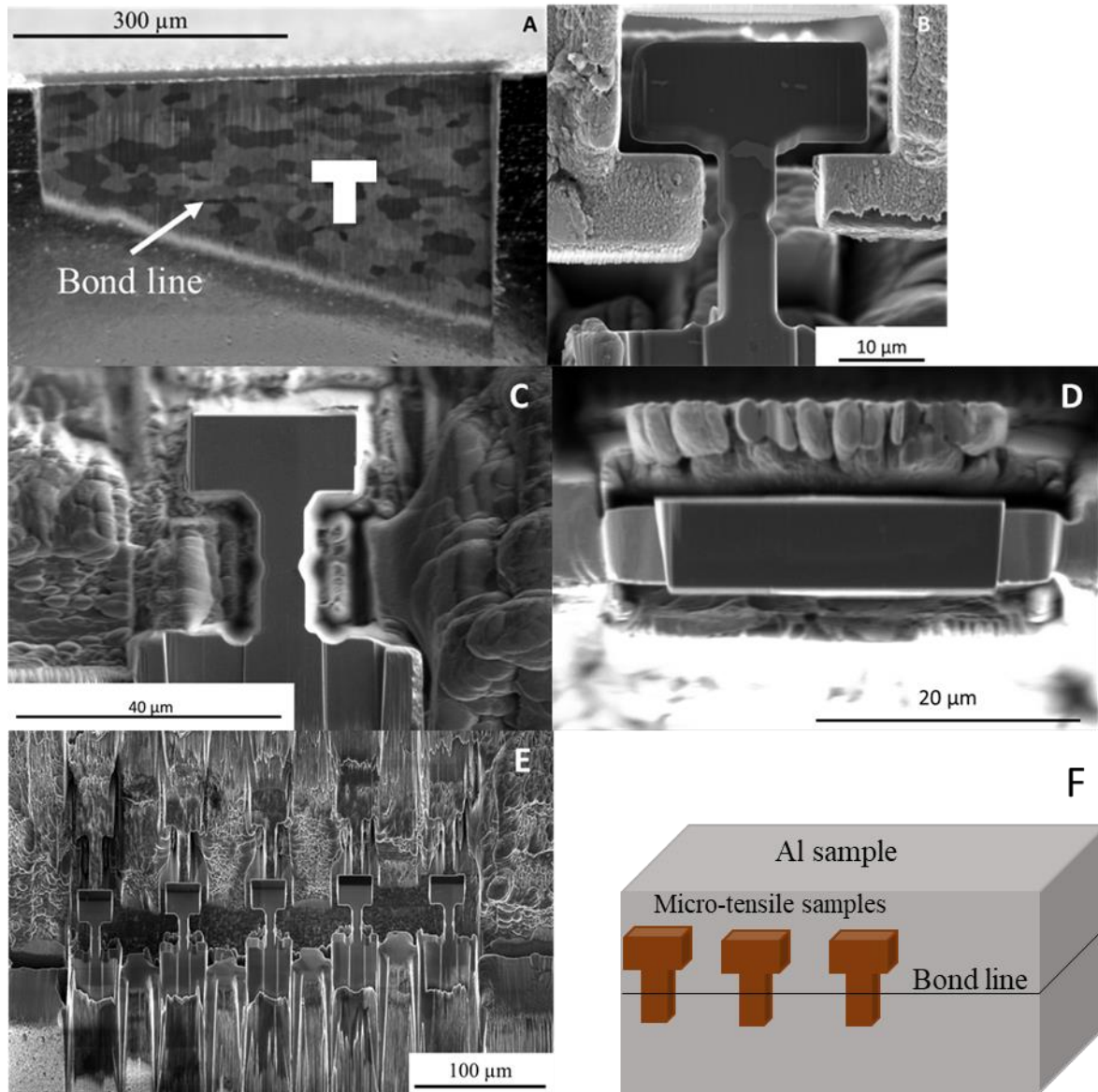


Figure 2: A) An SEM image of the microstructure illustrating the grain size. The bond line location and a schematic showing the location of the tensile bars is also included and not drawn to scale. B) An example of finished micro-tensile with gripper being aligned for testing. C) An example of a finished micro-tensile specimen side view showing the dimensions. D) An example of a finished micro-tensile specimen from the top view showing the thickness of micro-tensile bar. E) A group of finished micro-tensile bars ready for testing. F) A schematic showing the location of the micro-tensile bars.

The irradiated sample is from the top cladding portion of a plate that was irradiated to  $8.9 \times 10^{20}$  fissions/cm<sup>3</sup>. The micro-tensile specimens were tested at room temperature utilizing a Hysitron PI-88 picoindenter inside a FEI quanta dual beam (FIB/SEM) instrument. A custom-made gripper was manufactured in a diamond tip for tensile testing as seen in Figure 2B. During the testing of the micro-tensile bars the SEM beam was used to take pictures and record videos to enable post testing analysis (see supplemental information). The micro-tensile bars were tested with the PI-88

displacement control with displacement rates between 20-2000 nm/s which corresponds to strain rates of approximately  $0.001-0.1 \text{ s}^{-1}$ . The fracture surfaces of the micro-tensile bars after testing were examined with the SEM when possible.

## Results

The Hysitron PI-88 records the load versus displacement of the micro-tensile test. The load versus displacement data is then converted to engineering stress and strain using the dimensions of the micro-tensile specimen measured in ImageJ from the before images of each micro-tensile specimens. Examples of these images can be seen in Figure 2C and 2D. The stress is calculated from the cross-sectional area at the thinnest part of the gauge. This would be the narrowest part of the notch for the notched specimens. The strain is calculated from the displacement data and the total length of the gauge section. The yield stress was obtained from the stress versus strain curves using the 0.2 % offset method from the linear portion of the loading curves. The engineering stress versus strain curves for the 4 different samples can be seen in Figures 3-6. Table 1 contains the summarized results of the yield stress from the micro-tensile testing of the 4 samples with different displacement rates used.

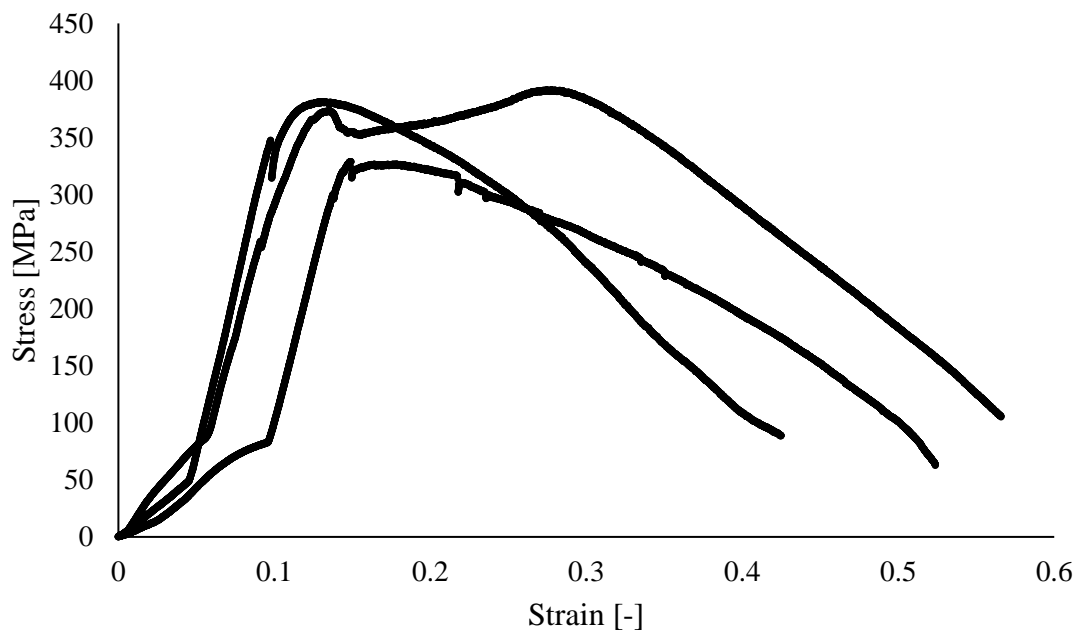


Figure 3: The stress versus strain curves for the Al control specimens. These micro-tensile specimens did not contain a bond line and were not notched. All 3 specimens on the Al control were tested at 200 nm/s at room temperature.

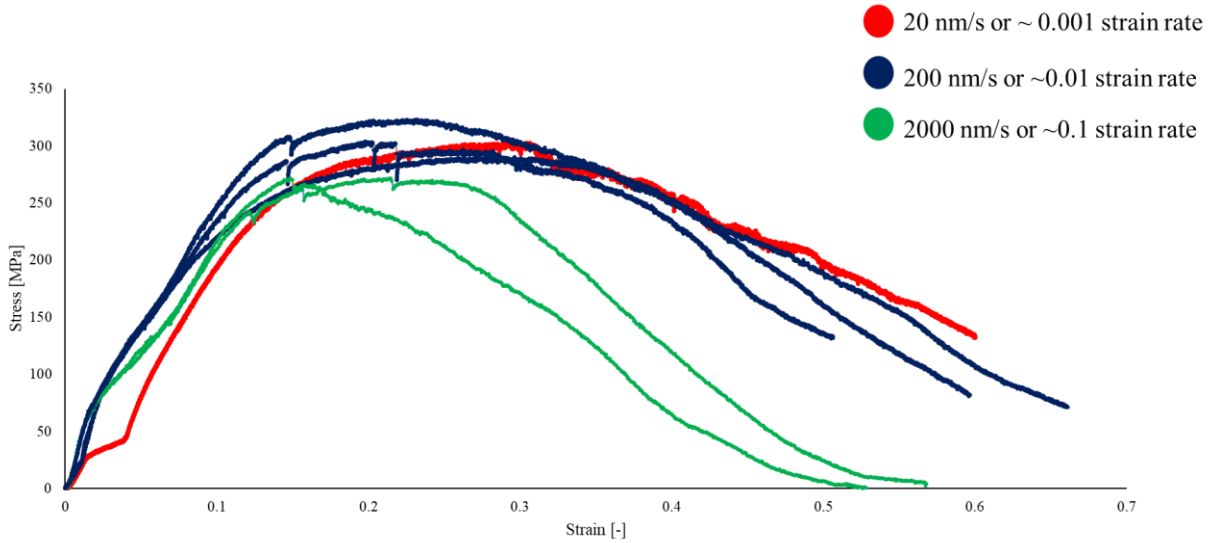


Figure 4: The Stress versus strain curves for the Al bond line 1. The micro-tensile specimens included the bond line and were notched. The color coding shows the different strain rates used ( $.001-1 \text{ s}^{-1}$ ). For this sample there were a total of 6 micro-tensile specimens tested as follows: 1 at 20 nm/s, 3 at 200 nm/s and 2 at 2000 nm/s.

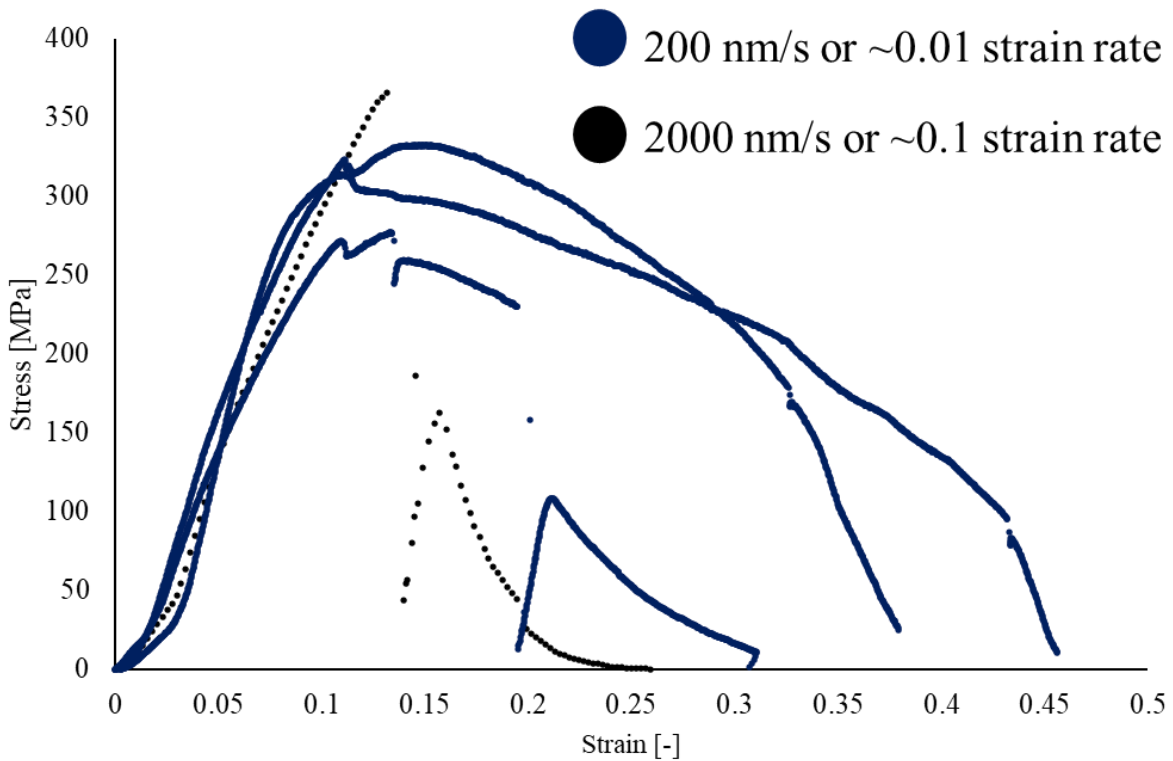


Figure 5: The stress versus strain curves for the Al bond line 2. These micro-tensile bars contained a bond line and were notched. There were a total of 4 micro-tensile bars tested on Al bond line as follows: 3 tested at 200 nm/s and 1 tested at 2000 nm/s.

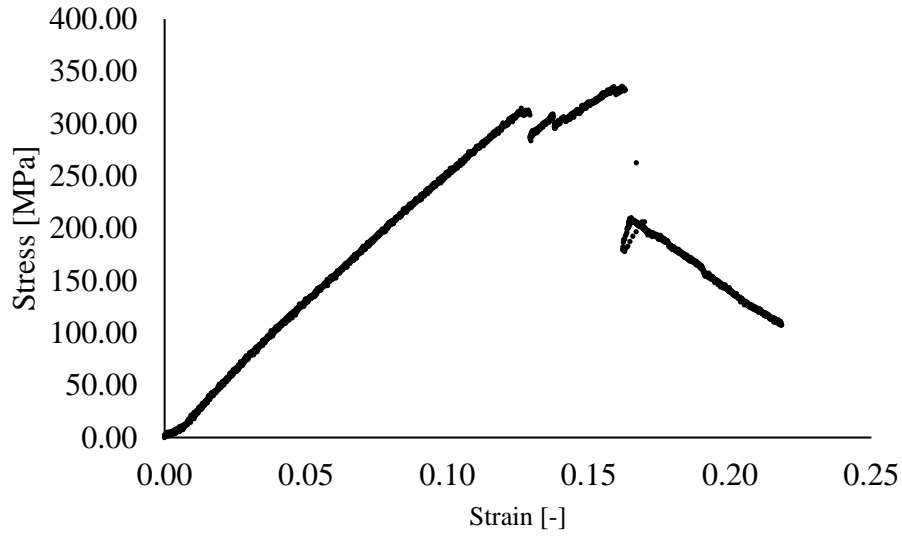


Figure 6: Neutron irradiated sample was pulled at 200 nm/s. This sample contained a bond line and was notched.

Table 1: The yield stress values of the micro-tensile tests performed on the samples with the displacement rates used.

Sample	Number of micro-tensile specimens	Displacement rate [nm/s]	Yield Stress [MPa]	UTS [MPa]	Uniform Elongation [-]
Al Control (AA 6061-T6)	3	200	302 ± 39	362 ± 30	.139 ± .009
Al bond line 1	1	20	211	300	.310
Al bone line 1	3	200	267 ± 44	305 ± 15	.248 ± .042
Al bond line 1	2	2000	238 ± 12	272 ± 1	.182 ± .045
Al bond line 2	3	200	299 ± 20	310 ± 30	.131 ± .019
Al bond line 2	1	2000	366	366	.132
Irradiated	1	200	323	333	.163

## Discussion

The non-irradiated materials containing the bond lines were tested at a variety of different strain rates for the micro-tensile specimens. Reviewing current literature indicates that there is little effect from strain rate on the deformation of 6XXX series Al alloys in the range tested [28, 29]. While the micro-tensile specimens would have many factors affect the yield strength of the individual tests it would appear from the results of Al bond line 1 that strain rate does not have significant influence on the results.

The advantage of performing the tests in-situ in the SEM permits the observation of the deformation in real time. Videos of selected tests can be seen in the supplementary material. In examining the results of the Al bond line 1 and Al bond line 2 micro-tensile specimens containing the bond line, in most cases the micro-tensile specimen failed in the aluminum grains surrounding the bond line in a ductile mode as seen in Figure 7.

In testing the control Al micro-tensile specimens with similar cross-sectional areas as the bond line specimens and despite not being notched, all have similar yield stress values. The Al control samples was a 6061-Al with T6 treatment which has yield strength values between 240-290 MPa. The value of  $302 \pm 39$  is slightly higher than the previously mentioned range but since these are small scale tests it can be expected. This agrees with the observations from literature from macro scale testing [30-36] where the optimized HIP bonded materials have similar properties to the as-received material. This demonstrates that an optimized HIP process does not significantly alter the mechanical properties of the aluminum.

Preliminary results and comparisons with the available literature indicate that materials bonded with an optimized HIP process produced adequate bonds with the bond line not being the limiting feature [30-36]. HIP bonded F82H steel [33] or reduced activation ferritic martensitic steels [35] for fusion applications also indicated that the macro-scale tensile specimens containing the bond line had similar yield, UTS and elongation characteristics when compared with as-received materials tensile specimens. In addition, the macro-scale tensile specimens did not fracture at the bond interface. A similar deformation behavior is evident with the micro-tensile specimens in the Al control sample which produced similar yield stress values as those micro-tensile specimens in Al bond line 1 and Al bond line 2. Most of the micro-tensile specimen in Al bond line 1 and Al bond line 2 samples did not fracture at the bond line and instead deformed in the aluminum around the bond line similar to the deformation in the macro-scale testing. While there may be challenges with size effects causing an increase in the yield stress measured with the micro-tensile specimens it is promising that the deformation mechanisms at the micro-scale agree with the macro-scale tests in literature [30-36]. This is beneficial allowing for a better understanding of the potential failure of the aluminum cladding in these fuel plates.

As described in literature concerning irradiated HIP bonded F82H steel it is reported that the irradiation did not cause fracture at the bond line [37]. However, in this research the micro-tensile specimen on the irradiated sample failed at the bond line. Because only a single irradiated specimen was tested in this research, it would be difficult to draw any meaningful conclusions. The irradiated specimen did have a higher yield strength as compared with most of the unirradiated specimens tested at the same displacement rate. It is expected that irradiation would increase the yield strength of the material through the damage in the material. The results from this research indicate that the yield strength of the Al control (as received) increases  $\sim 7\%$  when compared to the irradiated specimen. For the single irradiated micro-tensile results which are displayed in Figure 8 there was little to no deformation in aluminum around the bond line. It is known that the irradiation increases the defect density in the aluminum, which leads to an increase in strength of aluminum causing the bond line to become the weakest component. This resulted in a brittle fracture at the bond line under load. Aluminum alloys show rapid hardening even with low doses of neutron irradiation

[38] which could lead to the bond line becoming the weak layer. Another consideration is that when aluminum oxide (potential oxide at the bond line) is neutron irradiated at lower temperature  $\sim 400$  K it still maintains its crystalline structure [39] with small defect clusters and minimal swelling [39]. Since the bond line oxide is minimally affected by the irradiation it is possible that the increase in yield strength of the Al from irradiation would play a larger role in post irradiation deformation. This would suggest that the micro-tensile specimens would start to fail at the bond line after irradiation. It is difficult to draw any conclusions with only a single test specimen at a single dose for comparison to the unirradiated specimens. Additional, systematic studies with a variety of irradiated samples would be needed to thoroughly understand the change in the deformation behavior.

It is worth noting that one micro-tensile specimen in the unirradiated case failed by brittle fracture at the bond line, the fracture can be viewed in Figure 9. It was in Al bond line 2 which was tested at the highest displacement rate of 2000 nm/s. The bond line in the specimen failed at a stress of 366 MPa. While the other unirradiated micro-tensile specimens failed in a ductile manner within the Al around the bond line this micro-tensile specimen failed in brittle manner at the bond line of the material. No reason for this change in deformation behavior was evident. There was no precipitate in the micro-tensile bar nor did the bond line appear to be thicker in this region as compared with the other micro-tensile specimens. In addition, the other micro-tensile bar tested at 2000 nm/s in the Al bond line 2 sample failed in the aluminum around the bond line in a ductile mode similar to the lower displacement rate samples. Aluminum does have some anisotropy in its mechanical properties [40, 41] which could be affecting the deformation behavior in this instance. Unfortunately, electron backscatter diffraction (EBSD) was not performed on the micro-tensile bars before testing. The EBSD could have given the orientation of the aluminum grains around the samples, which would have indicated if the grains were orientated in stronger or weaker directions. Possibly the grains were orientated in stronger directions on either side of the bond line in this tensile specimen. These stronger grains could have resulted in enough stress to accumulate and cause a fracture along the bond line before the yielding of the aluminum grains around the bond line. This seems plausible as this specimen failed at a higher stress than the single irradiated micro-tensile specimen (366 MPa vs 323 MPa). The post fracture examination of this specimen which failed at the bond shows the typical cleavage fracture (Figure 9 C and D) expected with the brittle fracture of materials and limited to no deformation in the Al surrounding the bond line.

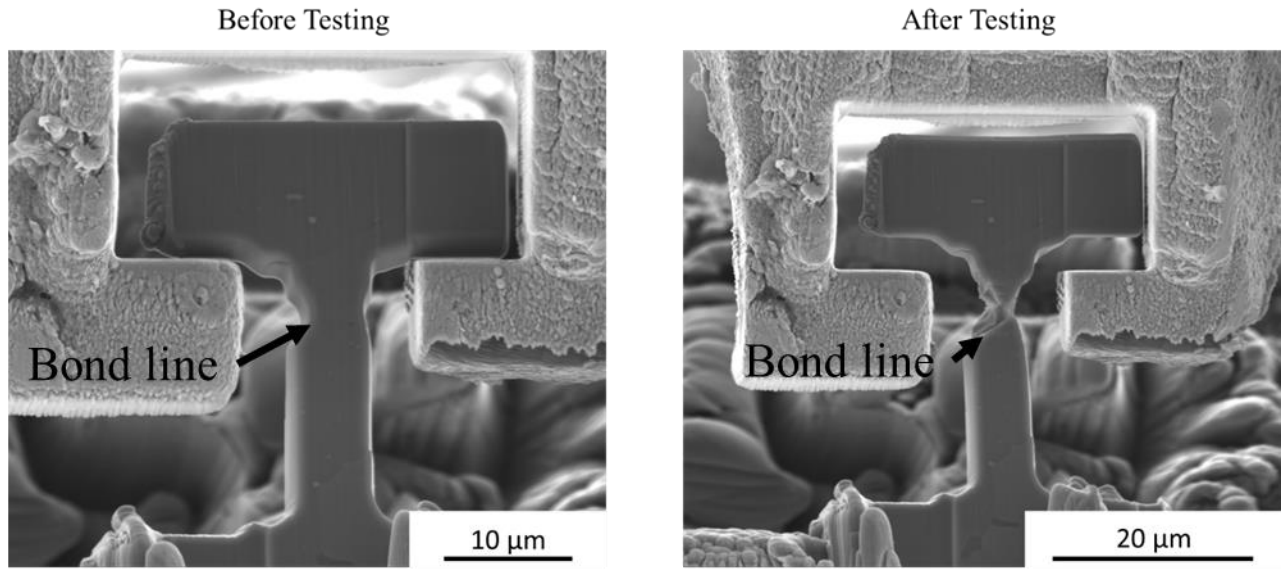


Figure 7: An example of an unirradiated micro-tensile bar (Al bond line 1) where the failure occurred in the ductile mode in the aluminum around the bond line. The SEM images were captured in secondary electron mode.

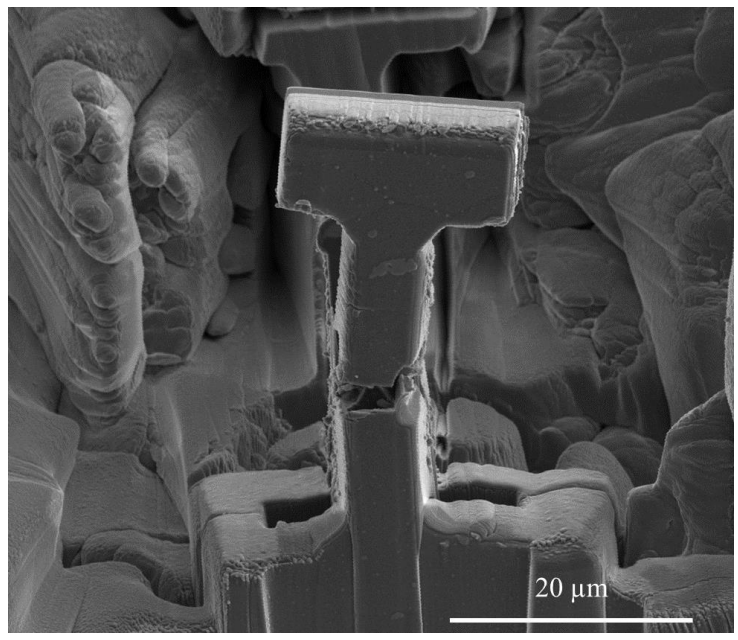


Figure 8: A SEM secondary electron image of after testing of the neutron irradiated specimen micro-tensile specimen.

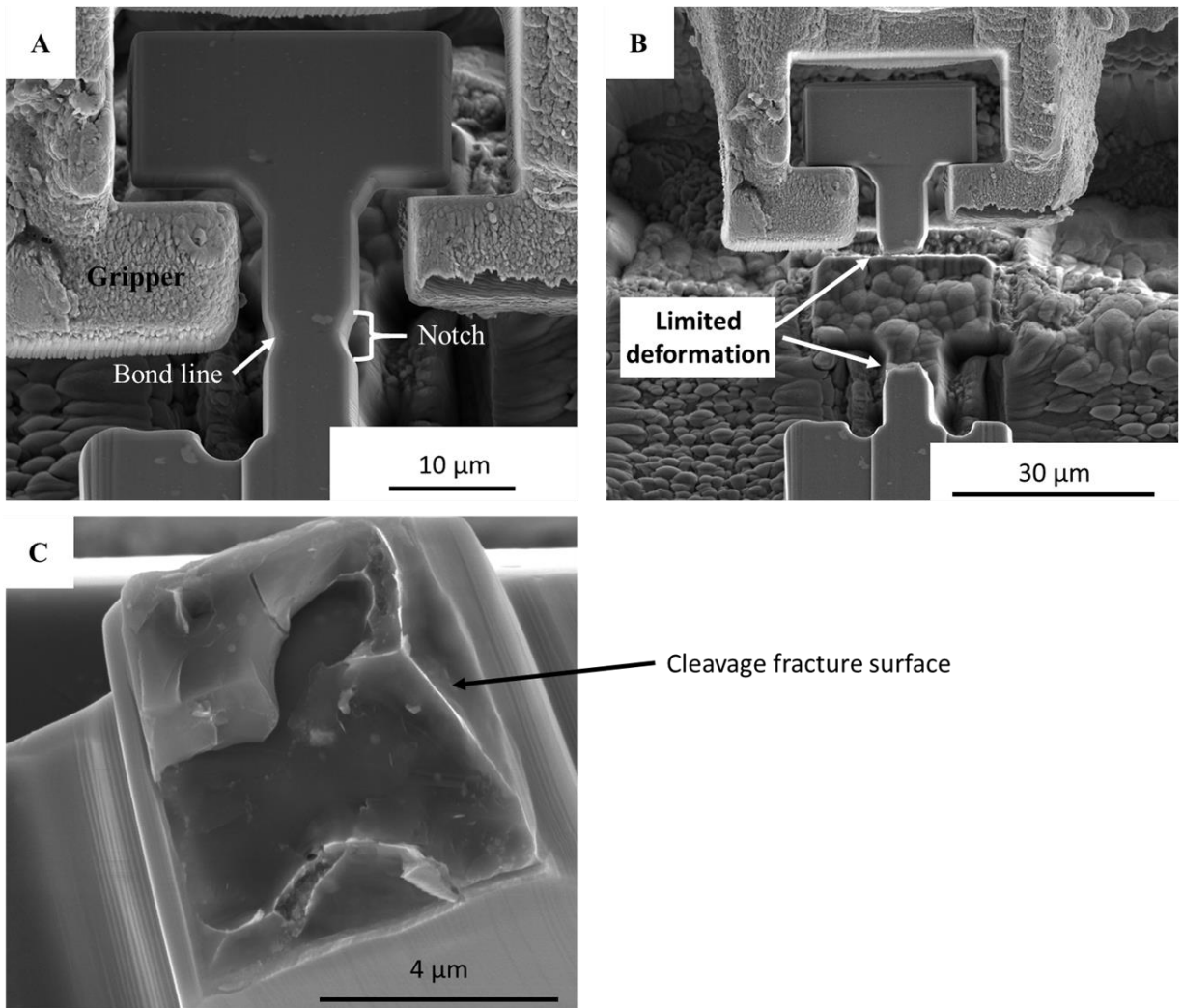


Figure 9: SEM secondary electron images of tensile 2 of the Al line bond 2 sample tested at 2000 nm/s A) The before image of testing the specimen. B) The after image of tested specimen. C) Fracture surface image of the specimen.

An additional benefit of small-scale mechanical testing is the ability to isolate microstructural features for testing as seen in Figure 10 with a precipitate in the middle of the micro-tensile bar. In Figure 10 images of the micro-tensile specimen in the Al bond line 1 sample that was tested at a displacement rate of 200 nm/s and yielded at 305 MPa. The images and supplementary videos indicate that the precipitate did not significantly affect the results of the micro-tensile test. This micro-tensile specimen has a similar yield strength value as compared with all the other unirradiated micro-tensile specimens tested at 200 nm/s. The precipitate does not appear to initiate the failure in the material or be the cause of the failure such as a crack initiation point. The micro-tensile bar in this case failed in a ductile mode in the grains surrounding the bond line like the several other micro-tensile specimens tested in the unirradiated state. However, in the macro-scale case the material around the precipitates could be more constrained which might lead to a different deformation behavior. For micro-cantilevers manufactured containing the bond line the results in Ref. [16] indicate that microstructural features such as voids or precipitates influenced the yield

strength. In [16] when the micro-cantilever contained a void or precipitates it measured a lower yield strength. This conflicts with the findings of this testing as the micro-tensile specimen in Figure 10 yielded with a value of 307 MPa which is very consistent with values of the other micro-tensile specimens here. The variance in yield behavior could result from the geometry of the test specimens with the uniaxial stress state of the micro-tensile versus the more complex stress state of the micro-cantilever. In the micro-cantilever the highest stress and strain in tension would be at the top of the micro-cantilever where the void or precipitate is located. Whereas the micro-tensile would have a uniaxial stress state so it would not be concentrated at the precipitate location. This difference could explain the varying behavior between the two techniques. In addition, in Ref. [16] only one micro-cantilever was tested in each condition.

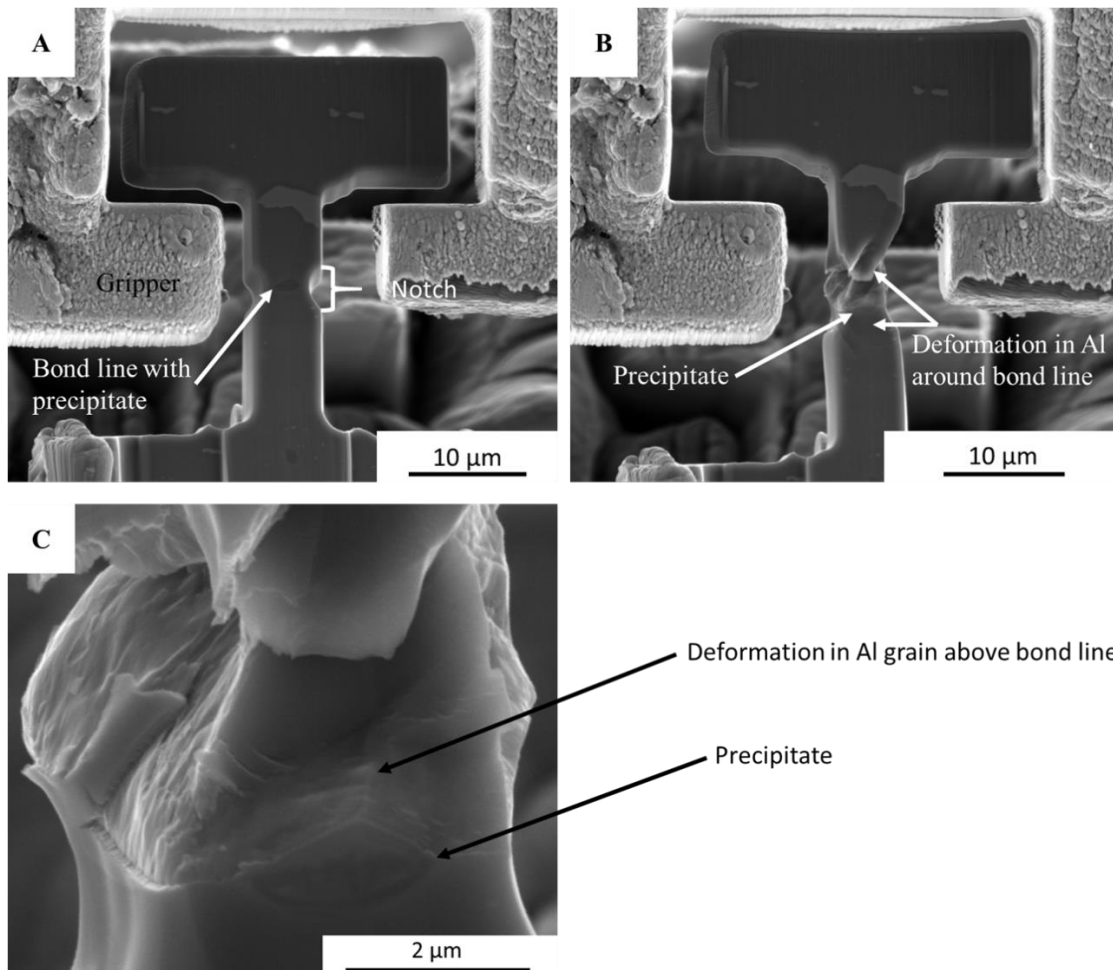


Figure 10: SEM secondary electron images of the testing of the micro-tensile specimen with a precipitate in the cross section. A) The before image of the testing of the micro-tensile specimen. B) The post testing image of the micro-tensile specimen. C) A SEM secondary electron image of the deformation region of the micro-tensile specimen after testing.

For a comparison of the size effect of the unirradiated micro-tensile specimens containing the bond line one can compare this data with data from the University of Central Florida [42] on HIP bonded Al. The macro-scale tensile tests also had a mix of results with some tensile bars failing at the bond

line and others in the matrix material. Macro-scale samples cooled in the furnace produced a similar microstructure of the bond line to the HIP processed plates. The yield stress was 82 MPa for the macro-scale sample which did not fail at the bond line and a value of 88.6 MPa for the macro-scale sample which did. In this study the value for the sample that did fail at the bond line in the unirradiated condition is 366 MPa. The average value for the other case (all different strain rates) of the micro-tensile specimens that did not fail at the bond line is 277 GPa. In this case a similar trend is observed with the sample fracturing at the bond line having a higher yield value as compared with specimens deforming in the aluminum around the grain. Furthermore, the macro scale specimens in [42] that were water quenched, which causes the Al matrix to develop increased hardness, failed [43] at the bond line more frequently. While water quenching is not the same as irradiation damage a similar trend is observed in both cases: when the Al matrix yield stress increases there is also an increase in failures at the bond line of the specimens. In [18] mm size tensile specimens were manufactured from HIPed bond Al containing a bond line and the yield strength was measured to be 255-275 MPa depending on the HIPing parameters. This is lower than values measured here which could be from several factors such as size effects in the material and differences in the HIPing of the materials. However, there was no comparison to irradiated material in this study.

## **Conclusions**

In literature [30-36] it was shown through macro-scale mechanical testing that materials bonded with the optimized HIP parameter have similar mechanical properties to the as-received material. Additionally, macro-scale mechanical testing revealed that neutron irradiated specimens [37] did not fail because of the bond line. In this micro-scale test the samples containing the bond line and those in the control Al sample had similar mechanical properties. Furthermore, the micro-tensile specimens enable the testing of the individual component or feature in the as-fabricated fuel plate. The unirradiated micro-tensile specimens tested here deformed in the Al surrounding the bond line indicating that a well adhered and strong bond line with all but one specimen. The Al control micro-tensile specimens had similar yield strength to the micro-tensile in Al bond line 1 and Al bond line 2 samples. The micro-tensile specimens showed that precipitates at the bond line do not appear to have affected the mechanical properties significantly. The micro-tensile specimens that contain a precipitate on the bond line did not deform differently than those without a precipitate on the bond line. The irradiated micro-tensile test showed a brittle fracture at the bond line with no deformation in the Al, suggesting that irradiation is causing a change in the deformation of the material due to the increase in the yield strength of the Al matrix. The micro-tensile tests performed here demonstrate the ability of small-scale mechanical testing to provide meaningful information on the individual as-fabricated components in order to improve the understanding of the deformation of the overall fuel plate.

## **Acknowledgements**

This submitted manuscript was authored by a contractor of the U.S. Government under DOE Contract No. DE-AC07-05ID14517. Accordingly, the U.S. Government retains and the publisher, by accepting the article for publication, acknowledges that the U.S. Government retains a nonexclusive, paid-up, irrevocable, world-wide license to publish or reproduce the

published form of this manuscript, or allow others to do so, for U.S. Government purposes. The funding for this work was provided by the USHPRR Project, Office of Material Management and Minimization National Nuclear Security Administration from the U.S. Department of Energy under DOE-NE Idaho Operations Office Contract DE-AC07-05ID14517. Authors would like to acknowledge the staff of the Electron Microscopy Laboratory (EML) at the Materials and Fuels Complex (MFC) at Idaho National Laboratory for their effort in handling, preparing, and transferring of the specimens used in this work.

## References

- [1] J.G. Stevens “Research Reactor Conversion to Low Enriched Uranium (LEU) Fuel” Reference Module in Earth systems and environmental sciences 2021
- [2] R. Prabhakaran, L. Gardner, V. Joshi, D. Burkes, C. Lavender “Effect of homogenization and hot rolling on the mechanical properties, microstructure and corrosion behavior of U-10Mo monolithic fuel” *J. Nucl. Mater.* 527 (2019) 151804
- [3] J.L. Snelgrove, G.L. Hofman, M.K. Meyer, C.L. Trybus, T.C. Wienczek “Development of very-high-density low-enriched-uranium fuels” *Nucl. Eng. Des.* 178 (1997) 119-128
- [4] M.K. Meyer, G.L. Hofman, S.L. Hayes, C.R. Clark, T.C. Wienczek, J.L. Snelgrove, R.V. Strain, K.H. Kim “Low-temperature irradiation behavior of uranium-molybdenum alloy dispersion fuel” *J. Nucl. Mater.* 208 (2003) 221-236
- [5] D.D. Keiser Jr., W. Williams, A. Robinson, D. Wachs, G. More, D. Crawford “Detailed measurements of local thickness changes for U-7Mo dispersion fuel plates with Al-3.5Si matrix after irradiation at different power in the RERTR-9B experiment” *J. Nucl. Mater.* 494 (2017) 448-460
- [6] J.-Y. Oh, Y.S. Kim, Y.-W. Tahk, H.-J. Kim, E.-H. Kong, J.-S. Yim “Modeling a failure criterion for U-Mo/Al dispersion fuel” *J. Nucl. Mater.* 473 (2016) 68-74
- [7] G.Y. Jeong, Y.S. Kim, Y.J. Jeong, J.M. Park, D.-S. Sohn “Development of PRIME for irradiation performance analysis of U-Mo/Al dispersion fuel” *J. Nucl. Mater.* 502 (2018) 331-348
- [8] J. Gan, B.D. Miller, D.D. Keiser Jr., J.-F. Jue, J.W. Madden, A.B. Robinson, H. Ozaltun, G. Moore, M.K. Meyer “Irradiated microstructure of U-10Mo monolithic fuel plate at very high fission density” *J. Nucl. Mater.* 492 (2017) 195-203
- [9] Z. Illtis, S. Drouan, T. Blay, I. Zacharie, C. Sabathier, C. Onofri, C. Steyer, C. Schwarz, B. Baumeister, J. Allenou, B. Stepnik, W. Petry “Microstructural characteristics of a fresh U(Mo) monolithic mini-plate: Focus on the Zr coating deposited by PVD” *Nucl. Eng. Tech.* (2021)

- [10] F. Housaer, F. Vanni, M. Touzin, F. Beclin, J. Allenou, A. Lenaers, A.M. Yacout, H. Palancher, B. Stepnik, O. Tougait “Morphological characterization of the fresh ZrN coated UMo powders used in EMPIrE irradiation experiment: A practical approach” *J. Nucl. Mater.* 533 (2020) 152087
- [11] X. Iltis, I. Zacharie-Aubrun, H.J. Ryu, J.M. Park, A. Leenaers, A.M. Yacout, D.D. Keiser, F. Vanni, B. Stepnik, T. Blay, N. Tariesien, C. Tanguy, H. Palancher “Microstructure of as atomized and annealed U-Mo<sub>7</sub> particles: A SEM/EBSD study of grain growth” *J. Nucl. Mater.* 495 (2017) 249-266
- [12] A. Metha, L. Zhou, E.A. Schutz, D.D. Keiser Jr., J.I. Cole, Y. Shon “Microstructural Characterization of AA6061 Versus AA 6061 HIP Bonded Cladding-Cladding interface” *J. Phase Equilib. Diffus.* (2018) 39:246–254
- [13] D.E. Burkes, D.D. Keiser, D.M. Wachs, J.S. Larson, M.D. Chapple “Characterization of Monolithic Fuel Foil Properties and Bond Strength” Transactions for the International Topical Meeting on Research Reactor Fuel Management (RRFM), Lyon, France; March 2007
- [14] J.M. Wight, G.A. Moore, S.C. Taylor, N.E. Woolstenhulme, and S.T. McCormick “TESTING AND ACCEPTANCE OF FUEL PLATES FOR RERTR FUEL DEVELOPMENT EXPERIMENTS” RERTR 2008-30th INTERNATIONAL MEETING ON REDUCED ENRICHMENT FOR RESEARCH AND TEST REACTORS
- [15] C. Liu, M.L. Lovato, K.D. Clarke, D.J. Alexander, W.R. Blumenthal, “Miniature bulge test and energy release rate in HIPed aluminum/aluminum interfacial fracture” *J. Mech. Phys. Solids* 120 (2018) 179-198
- [16] N.A. Mara, J. Crapps, T.A. Wynn, K.D. Clarke, A. Antoniou, P.O. Dickerson, D.E. Dombrowski, B. Mihaila “ Microcantilever bend testing and finite element simulation of HIP-ed interface-free bulk AL and Al-AL HIP bonded interfaces” *Phil Mag.* 93 (2013) 2749-2758
- [17] D.D. Keiser Jr., J.-F. Jue, J. Gan, B.D. Miller, A.B. Robinson, J.W. Madden, M.R. Finlay, G. Moore, P. Medvedev, M. Meyer “ Microstructural characterization of an irradiated RERTR-6 U-7Mo/AA4043 alloy dispersion fuel plate specimen blister-tested to final temperature of 500 °C” *J. Nucl. Mater.* 488 (2017) 100-122
- [18] D.E. Burkers, F.J. Rice, J.-F. Jue, N.P. Hallinan “Update on mechanical analysis of monolithic fuel plates” Conference: 12th annual topical meeting on Research Reactor Fuel Management (RRFM) ,Hamburg, Germany,
- [19] A. Soulami, D.E. Burkes, V.V. Joshi, C.A. Lavender, D. Paxton “Finite-element model to predict roll-separation force and defects during rolling of U-10Mo alloys” *J. Nucl. Mater.*, 494 (2017), pp. 182-191
- [20] H. Ozaltun, M.-H. Herman Shen, P. Medvedev “Assessment of residual stresses on U10Mo alloy based monolithic mini-plates during Hot Isostatic Pressing” *J. Nucl. Mater.*, 419 (2011), pp. 76-84

- [21] D. Frazer, D. Jadernas, N. Bolender, J. Madden, J. Giglio, P. Hosemann “Elevated temperature microcantilever testing of fresh U-10Mo Fuel” *J. Nucl. Mater.* 526 (2019) 151746
- [22] P. Hosemann “Small-scale mechanical testing on nuclear materials: bridging the experimental length scale gap” *Scripta Materialia* 143 (2018) 161-168
- [23] H.T. Vo, A. Reichardt, D. Frazer, N. Bailey, P. Chou, P. Hosemann “In situ micro-tensile testing on proton beam-irradiated stainless steel” *J. Nucl. Mater.* 493 (2017) 336-342
- [24] Jan-Fong Jue, Blair H. Park, Curtis R. Clark, Glenn A. Moore and Dennis D. Keiser, Jr., “Fabrication of Monolithic RERTR Fuels by Hot Isostatic Pressing,” *Nuclear Technology*, 172 204-210 (2010).
- [25] Jan-Fong Jue, Dennis D. Keiser, Jr., Cynthia R. Breckenridge, Glenn A. Moore, and Mitchell K. Meyer, “Microstructural Characteristics of HIP-bonded Monolithic Nuclear Fuels with a Diffusion Barrier,” *Journal of Nuclear Materials*, 448 250-258 (2014).
- [26] J.I. Cole, J-F Jue, G.A. Moore, G.A., 2021. Fuel Design and Fabrication: Research Reactor Fuel. In: Greenspan, E. (Ed.), *Encyclopedia of Nuclear Energy*, vol. 2. Elsevier, pp. 326–333. <https://dx.doi.org/10.1016/B978-0-12-819725-7.00125-2>.
- [27] Y. Xiao, V. Maier-Kiener, J. Michler, R. Spolieriak, J.M. Wheeler “Deformation behavior of aluminum pillars produced by Xe and Ga focused ion beams: Insights from strain rate jump tests” *Mater. Des.* 181 (2019) 107914
- [28] E. Cadoni, M. Dotta, D. Forni, H. Kaufmann “Effects of strain rate on mechanical properties in tension of a commercial aluminium alloy used in armour applications” *Procedia structural integrity* 2 (2016) 986-993
- [29] X. Chen, Y. Peng, S. Peng, S. Yao, C. Chen, P. Xu “Flow and fracture behavior of aluminum alloy 6082-T6 at different tensile strain rates and triaxialities” *PLoS ONE* 12(7): e0181983
- [30] S. Stao, T. Hatano, T. Kuroda, K. Furuya, S. Hara, M. Enoeda, H. Takatsu “Optimization of HIP bonding conditions for ITER shielding blank/first wall made from austenitic stainless steel and dispersion strengthened copper alloy” *J. Nucl. Mater.* 528-263 (1998) 265-270
- [31] C. Li, Q. Huang, P. Zhang, FDS Team, “Preliminary experimental study on Hot Isostatic Pressing diffusion bonding for CLAM/CLAM” *Fus. Eng. Des.* 82 (2007) 2627-2633
- [32] H.-S. Wang, Y.-L. Kuo, C.-M. Kuo, C.-N. Wei “Microstructural evolution and mechanical properties of hot isostatic pressure bonded CM 247LC superalloy cast” *Mater. Des.* 91 (2016) 104-110
- [33] K. Furuya, E. Wakai, M. Ando, T. Sawai, A. Iwabuchi, K. Nakamura, H. Takeuchi “Tensile and impact properties of F82H steel applied to HIP-bond fusion blanket structures” *Fus. Eng. Des.* 69 (2003) 385-389

- [34] T. Hirose, K. Shiba, M. Ando, M. Enoeda, M. Akiba “Joining technologies of reduced activation ferritic/martensitic steel for blanket fabrication” *Fus. Eng. Des.* 81 (2006) 645-651
- [35] J.-S. Lee, J.-Y. Park, B.-K. Choi, B.G. Hong, K.-J. Jung, Y.H. Jeong “HIP Joining of RAFM/RAFM Steel and Beryllium/RAFM Steel for Fabrication of the ITER TBM First wall” *Met. Mater. Int.* 15 (2009) 456-470
- [36] D.Y. Ku, S. Oh, M.-Y. Ahn, I.-K. Yu, D.-H. Kim, S. Cho, I.-S. Choi, K.-B. Kwon “TIG and HIP joining of Reduced Activation Ferrite/martensitic steel for Korean ITER-TBM” *J. Nucl. Mater.* 417 (2011) 67-71
- [37] F. Kazuyuki, W. Eiichi, M. Kenji, A. Masato, S. Masayoshi “Effects of irradiation on mechanical properties of HIP-bonded reduced-activation ferritic/martensitic steel F82H first wall” *J. Nucl. Mater.* 367-370 (2007) 494-499
- [38] M. Kolluri “Neutron Irradiation Effects in 5xxx and 6xxx Series Aluminum Alloys: A Literature Review”
- [39] F.W. Clinard, G.F. Hurley, L.W. Hobbs “ Neutron irradiation damage in MgO, Al<sub>2</sub>O<sub>3</sub> and MgAl<sub>2</sub>O<sub>4</sub> ceramics” *J. Nucl. Mater.* 108 & 109 (1982) 655-670
- [40] M. Tajally, E. Emadoddin “Mechanical and anisotropic behaviors of 7075 aluminum alloy sheets” *Mater. Des.* 32 (2011) 1594-1599
- [41] W.F. Hosford “The anisotropy of aluminum and aluminum alloys” *JOM* 58 (2006) 70-74
- [42] A. Mehta and Y. Sohn “Mechanical behavior of Diffusion Bonded Interface of Aluminum Alloy 6061” Report to INL
- [43] G. P. Dolan, R. J. Flynn, D. A. Tanner & J. S. Robinson (2005) Quench factor analysis of aluminium alloys using the Jominy end quench technique, *Materials Science and Technology*, 21:6, 687-692, DOI: 10.1179/174328405X43081